Mineral Analysis of Dolomite Formation During Carbonate Acidizing Using Chelating Agents

Mian Umer Shafiq, Nazarbayev University, Astana, Kazakhstan; **Hisham Ben Mahmud,** UTP Malaysia; **Bandar Seri Iskander,** Ipoh, Malaysia; **Lei Wang,** Chengdu University of Technology, China; **Maryam Jamil,** Shenzhen University, Shenzhen, China; **Sophia Nawaz Gishkori,** University of Gujrat, Gujrat, Pakistan

Abstract

During carbonate acidizing, the reaction between hydrochloric acid (HCl) and carbonate minerals is particularly rapid, especially in high-temperature wellbore environments. Due to the swift reaction kinetics and the rapid consumption of acid, deep penetration is often limited, resulting in the formation of small wormholes and localized dissolution, which minimizes skin damage. To address these challenges, chelating agents have been introduced as an alternative for reacting with dolomite formations. Chelating agents, being slower-reacting acids, have demonstrated effectiveness in high-temperature environments. In this study, three chelating agents—HEDTA (Hydroxyethylenediaminetetraacetic acid), GLDA (L-glutamic acid diacetic acid), and EDTA (Ethylenediaminetetraacetic acid)—were employed to interact with Guelph dolomite core samples under high-pressure (1000 psi) and high-temperature (180°F) conditions. The reacted dolomite samples were subsequently analyzed for changes in various properties, including mineralogy, grain size distribution, porosity, and morphology. Mineralogical and grain size distribution analyses revealed that GLDA and HEDTA were effective in dissolving calcite, while EDTA demonstrated a higher effectiveness in dissolving ankerite. Additionally, mineral locking analysis indicated that GLDA and HEDTA successfully disrupted the bond between quartz and calcite, which may contribute to an increase in reservoir permeability.

Introduction

In sandstone acidizing, the primary objective is to remove or dissolve fine particles and other damage that cause bridging or blockages within the pore spaces. In carbonate reservoirs, which are primarily acid-soluble, acidizing operations typically create conductive pathways referred to as "wormholes." These wormholes serve as highly permeable flow paths, significantly enhancing hydrocarbon flow (Ghommem et al. 2015; Wilson 2016). In these formations, carbonates are expected to dissolve completely at slow injection rates near the wellbore (Fredd and Fogler 1998). However, the use of hydrochloric acid (HCl) in carbonate acidizing presents several drawbacks, including excessive corrosion, insufficient etching duration, and the formation of oil sludge due to crude asphaltenes. The following sections will discuss some of the acids developed over recent decades for matrix acidizing, highlighting their benefits and limitations.

Experimental studies have demonstrated the influence of various factors on matrix acidizing, such as the injection rate of acid, rock properties, the acid's reaction rate with the rock, permeability, porosity, mineralogy, pore structure, and mineral distribution (Qiu et al. 2011; Maheshwari and Balakotaiah 2013). Over the past few

decades, matrix acidizing has been extensively applied to treat formations such as low-temperature reservoirs (<100°C), clean sandstones (<10% dolomite), and clean dolomites (Morgenthaler 2013). However, reservoirs with these properties are increasingly rare. Today, deeper, hotter, and more heterogeneous reservoirs with complex mineralogies require acidizing treatment. To enhance the effectiveness of acidizing in both sandstone and carbonate formations and mitigate the adverse effects of precipitation, the development of new technologies is essential.

The behavior of foam and its impact on porous carbonate formations has been extensively studied (Ettinger and Radke 1992). They investigated the in-situ generation of foam during carbonate acidizing in a 1-ft long sample, which facilitated deeper penetration into the formation and the creation of deeper wormholes. As a result, this method uses less acid compared to conventional techniques. This foam-assisted acidizing technique enhances the wormhole formation process, while also allowing for the use of lower acid flow rates in areas prone to face dissolution. The in-situ foam generation is particularly effective in formations where low acid injection rates are required, or in heterogeneous formations where some zones accept acid more slowly. The foam system is especially well-suited for low-permeability formations, such as dolomites (Hoefner, 1987), as it confines the acid to the primary flow path, ensuring efficient acid utilization within that channel. At a flow rate of 0.25 cm³/sec, conventional stimulation resulted in the dissolution of most of the core, leading to a significant increase in permeability. Therefore, the foam system proves to be highly efficient in generating wormholes.

Additionally, low-carbon steel tubes may develop rust that could be damaged by hydrochloric (HCl) acid. The HCl acid can break down this rust, releasing iron ions (Fe^{3+}), which may precipitate and potentially harm the reservoir and production well. According to Gdanski (1998) and Nasr-El-Din et al. (2002), mud acid decomposes quickly at the wellbore due to the rapid reaction, resulting in the formation of precipitates and limiting acid penetration into the formation.

Limited research has been conducted on carbonate acidizing due to its relatively straightforward nature, but in recent years, substantial progress has been made in understanding this process (Shafiq and Mahmud 2017; Hassan and Al-Hashim 2017; Shafiq et al. 2023). The matrix acidizing process in carbonate formations differs significantly from sandstone acidizing, primarily because the entire carbonate rock is reactive, whereas in sandstone, only a small portion is reactive. This leads to the formation of large flow channels (depending on pore size) in certain areas of the rock, while other areas remain unaffected. This dissolution pattern results from the heterogeneous nature of carbonate formations. Since the pore sizes in carbonates are often macroscopic, these conductive channels can accommodate high-flow rates of fluid, thereby significantly increasing the permeability of the rock. In contrast, sandstone stimulation generally leads to a homogeneous permeability increase throughout the sample due to pore-scale dissolution across the entire rock (Bernadiner 1992).

Nasr-El-Din et al. (2007) developed an acidic chelate-based mixture aimed at mitigating secondary and tertiary reactions, providing long-lasting effects in sensitive sandstone formations. However, the application of these chelates is generally limited to high-temperature formations with high dolomite content and low clay content.

The response of dolomite to acidizing differs from that of limestone formations due to the temperature-dependent reaction between dolomite and hydrochloric acid (HCl) (Hoefner 1987). Previous studies have indicated that dolomite formations experience more dissolution compared to limestone. Carbonate rocks, which are sedimentary in nature, are primarily composed of carbonate minerals, including limestone ($CaCO_3$) and dolomite ($CaMg(CO_3)_2$). These minerals tend to react rapidly with HCl or other acids, creating wormholes even under low-temperature conditions. The process of wormhole formation is illustrated in **Figure 1**.
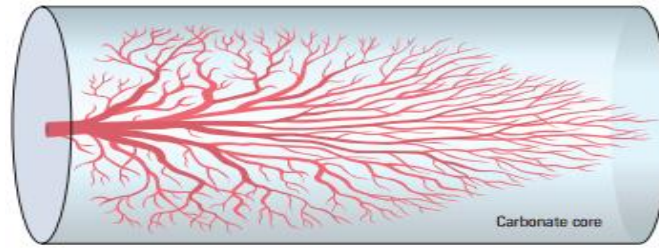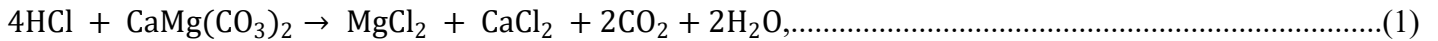
Figure 1—Wormhole pattern in dolomite acidizing (Al-Harthy 2009).

Eq. 1 represented the mechanism of reaction between HCl and dolomite.

$$4HCl \ + \ CaMg(CO_3)_2 \rightarrow \ MgCl_2 \ + \ CaCl_2 \ + 2CO_2 + 2H_2O, \dots\dots\dots\dots\dots\dots\dots\dots\dots\dots\dots\dots\dots\dots\dots\dots\dots(1)$$

Thus, the existence of wormholes in dolomite formation is the reason for productivity increment which is formed in the near wellbore region by formation dissolution and creation of new flow paths but not by removing the formation damage like in sandstone formation. According to Hawkins (1990), the formula for skin factor is mentioned in **Eq. 2**.

$$s = \left(\frac{k}{k_s} - 1\right) \ln \left(\frac{r_s}{r_w}\right), \dots\dots\dots\dots\dots\dots\dots\dots\dots\dots\dots\dots\dots\dots\dots\dots\dots\dots\dots\dots\dots\dots\dots\dots\dots\dots(2)$$

where s is the skin in the simulated or damaged area; k_s is permeability; and r_s is the radius of the stimulated or damaged area around the wellbore.

If the value of k_s is very large compared to k, then k/k_s can be neglected. The value of wellbore radius (r_w) is constant for calculation; therefore, skin value is dependent on r_s. Therefore, a high r_s value represents a similar effect to negative skin which shows a stimulated zone (Buijse and van Domelen 1998). Conclusively, it can be said that narrow and long wormholes are better compared to wide and short ones to enhance reservoir production.
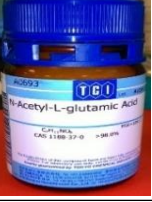
The application of chelating agents on sandstone and carbonate formations has developed as an effective enhanced oil recovery (EOR) technique (Shafiq et al. 2022). The thorough recovery mechanisms that are leading to significant oil recovery due to the use of these chemicals are not fully understood. However environmental issues and less dissolving power of these agents is the point of concern (Almubarak et al. 2017).

Methodology and Materials

To perform acidizing experiments, fluids, and core flooding apparatus were used that consist of the following parts and functions.

Fluids. During various stages of experimental work, three different types of fluids were utilized. These fluids used are different chelating agents like GLDA, HEDTA, and EDTA. Properties and descriptions of chelating agents used in this project are mentioned in **Table 1**.

Table 1—Chelating Agent and their properties.

Chelating Agent	Properties and Description
	It is a colorless amino polycarboxylic acid and is water soluble. It is used to remove limescale and it can sequester metal ions such as calcium and iron. It is being applied during acidizing due to its stability and less corrosive nature at high temperatures. The The most popular, powerful, economical, and all-purpose chelating agent. Disodium salt EDTA Disodium salt Density: 860 mg/mL[1] (at 20 °C), Formula: $C_{10}H_{16}N_2O_8$
	It is a colorless amino polycarboxylic acid. A chelating agent with similar effectiveness to EDTA. Very useful in the petroleum industry acidizing procedure to stabilize iron at a high pH value and is soluble at a low pH value. It has less corrosivity at high temperatures. Formula: $C_{10}H_{18}N_2O_7$
	The latest, strong, and green chelate. It is readily biodegradable and safe and can be used in cleaning applications, as an alternative to EDTA, phosphates, and phosphonates, it is good solubility over a broad pH spectrum. It is usually originating from a natural sustainable source. Formula: $C_9H_9NO_8Na_4$

Core Sample. The Guelph dolomite core samples utilized in this study were procured from Kocurek Industries INC, Hard Rock Division, located in Caldwell, Texas, USA. These samples exhibit inherent heterogeneity, with porosity and permeability characteristics tailored to meet specific experimental requirements. Petrophysical analysis indicates that the samples are well-sorted, clean formations demonstrating moderate porosity (17%) and very low permeability (10 md). It should be noted that due to the heterogeneous nature of the formation, these petrophysical properties may vary between individual core plugs.

Mineralogical composition analysis reveals that the Guelph dolomite is predominantly composed of ankerite (93-95%) and feldspar (3-5%), with trace amounts of calcite and aluminosilicates present. The cementing material primarily consists of quartz (85-90%), accompanied by clays (6-8%), dolomite (1-2%), and minor quantities of iron sulfide. For identification and reference purposes, the samples were systematically labeled using the nomenclature "Dolomite" followed by alphabetical designations (e.g., Dolomite A, Dolomite B). This classification system facilitates accurate tracking and comparison of experimental results across different samples.

Procedure. Core flooding tests were done to acidify the core sample. **Figure 2** shows how, after being placed inside the core holder, the core sample was contained at 1000 pressure using a syringe pump. The inlet and exit wings were made sure to be closed before confinement, and the intake wing was connected to the HPLC pump. Using heating tape and a temperature controller, the core holder is heated to the appropriate temperature of 180° F. One cc/min of acid was administered after the core holder had been heated for around 24 hours. The pressure changes at the input and output are measured using pressure transducers. Once the pressure drop was steady, the acid stopped flowing. The core sample was placed in the oven to dry for 24 hours after the confining pressure was removed and the fittings were unplugged.
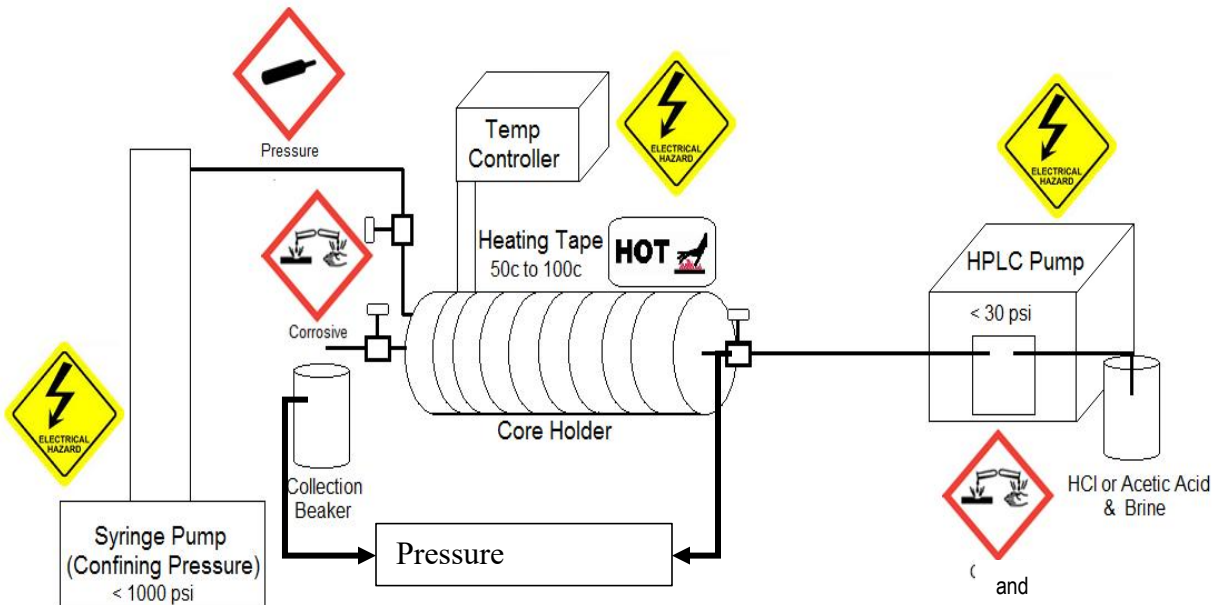
Figure 2—Core flooding setup (Shafiq et al. 2023).

Tescan Integrated Mineral Analysis (TIMA). TIMA is an advanced automated mineralogy system based on scanning electron microscopy (SEM), equipped with backscattered electron (BSE) imaging, cathodoluminescence (CL), and four energy-dispersive X-ray spectroscopy (EDS) detectors. This configuration enables rapid and high-resolution analysis of mineralogical and textural properties. TIMA provides comprehensive characterization capabilities, including mineral and elemental mapping, mineral associations, quantitative mineral abundance, porosity distribution, particle size analysis, and size-by-size liberation analysis. These features make it a powerful tool for reservoir rock characterization, process optimization, and geochemical studies. A notable application of this technique was demonstrated in the case study by Ward et al. (2017), which utilized TIMA to analyze grain size, mineral chemistry, texture, and mineralogical changes in the sedimentary deposits of Boodie Cave.

Procedure. The TIMA analysis begins with the preparation of a polished thin section, which is then imaged using backscattered electron (BSE) and energy-dispersive X-ray (EDX) techniques to identify individual mineral grains. Each mineral particle is scanned at a predefined resolution by multiple EDX detectors. The acquired EDX spectra are automatically compared against the TIMA mineral classification database, enabling precise mineral phase identification and high-resolution mineral mapping. For this study, the following analyses were performed using TIMA:

(1) Elemental Mass Analysis: Quantification of elemental composition.
(2) Element Behavior Analysis: Distribution and association of elements within the mineral matrix.
(3) Mineral Locking Analysis: Identification of mineral intergrowths and associations.
(4) Mineral Mass Analysis: Quantitative determination of mineral abundances.
(5) Mineral Location (Panorama): Spatial distribution of minerals within the sample.
(6) Grain Size Analysis: Measurement of individual grain dimensions.
(7) Particle Size Distribution: Statistical analysis of particle sizes.
(8) Density Distribution Analysis: Variation in mineral density across the sample.
(9) Porosity Distribution Analysis: Quantification and spatial distribution of porosity.

The analyses were conducted on sandstone and dolomite formations treated with two distinct acid systems. The first phase of the study focused on the interaction of pre-flush stage acids with the rock matrix, while the second phase evaluated the effects of chelating agents on mineral dissolution and texture alteration. A detailed discussion of each analysis and its results is presented in the following section.

Results and Discussion

This section presents a comprehensive analysis of the effects of three chelating agents on Guelph dolomite core samples. To evaluate the interaction of these chelates with all mineral phases present in the rock matrix, the experiments were conducted on unreacted Guelph dolomite core samples rather than preflushed samples. This approach ensures a clear understanding of the chelates' reactivity with the native mineralogy of the formation.

Elemental Analysis. Guelph dolomite is a carbonate rock primarily composed of ankerite, with heterogeneous permeability and porosity distributions. It also contains minor amounts of other carbonate minerals, such as calcite and dolomite. Due to its mineralogical homogeneity, the initial elemental composition of all core samples was consistent, providing a reliable baseline for comparative analysis.

Post-acidizing elemental analysis (**Figure 3**) revealed no significant changes in the elemental composition of the Guelph dolomite samples. This observation can be attributed to the dominance of ankerite, which acts as an insoluble matrix mineral in this formation. In contrast, the same chelating agents demonstrated effective dissolution of ankerite in sandstone formations, highlighting the mineral-specific reactivity of these chelates.

Despite the lack of significant elemental changes, further analyses were conducted to elucidate the reaction mechanisms between the chelating agents and the dolomite formation. These additional investigations provide critical insights into the chemical interactions and potential applications of chelates in carbonate reservoirs.
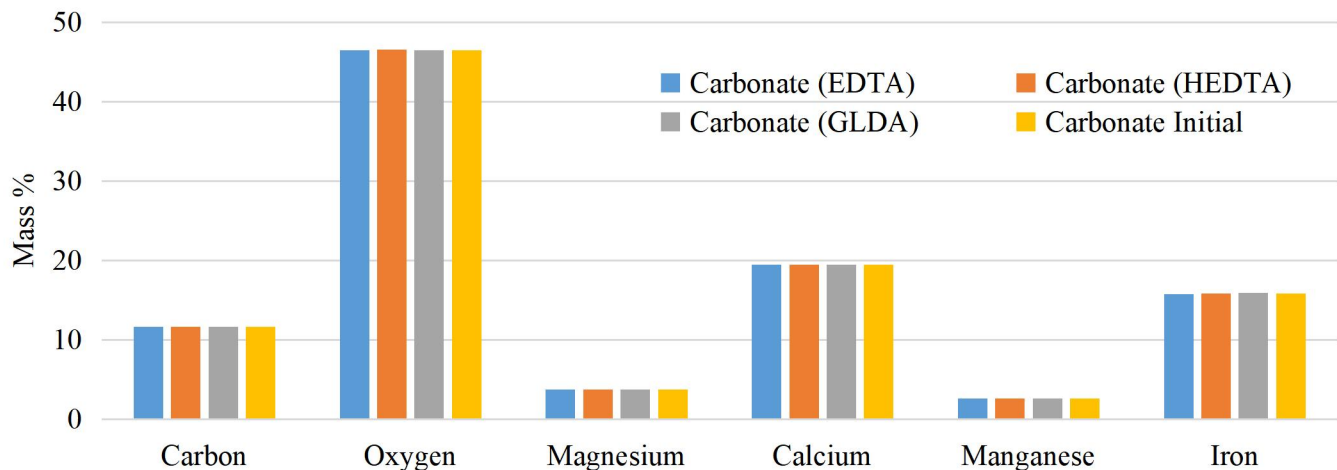

Figure 3—Guelph dolomite's elemental mass before and after its interaction with chelating chemicals.

Elemental Deportment Analysis. Elemental deportment refers to the distribution and association of specific elements within distinct mineral phases. **Figure 4** illustrates the deportment of calcium in the Guelph dolomite core sample, primarily hosted in dolomite and calcite minerals. The analysis revealed that GLDA (L-glutamic acid N,N-diacetic acid) demonstrated a higher capacity to dissolve calcium from both dolomite and calcite compared to the other chelating agents tested. This finding appears contradictory to the earlier elemental analysis, which indicated no significant changes in elemental composition.

This discrepancy can be explained by the relative nature of elemental analysis. In cases where one element dissolves while another remains unaffected, the relative percentage of the undissolved element increases. Conversely, if both elements dissolve in equal proportions, their relative mass percentages remain unchanged, masking the dissolution process in the overall elemental analysis.

Magnesium, another key element in the Guelph dolomite, is primarily hosted in ankerite and dolomite minerals. As previously discussed, ankerite exhibited negligible dissolution in the presence of all tested chelating agents. However, GLDA was observed to dissolve a small fraction of dolomite, as evidenced by the

results presented in **Figures 4** and **5**. This selective dissolution behavior underscores the mineral-specific reactivity of chelating agents and highlights the importance of deportment analysis in understanding chemical interactions at the mineralogical level.
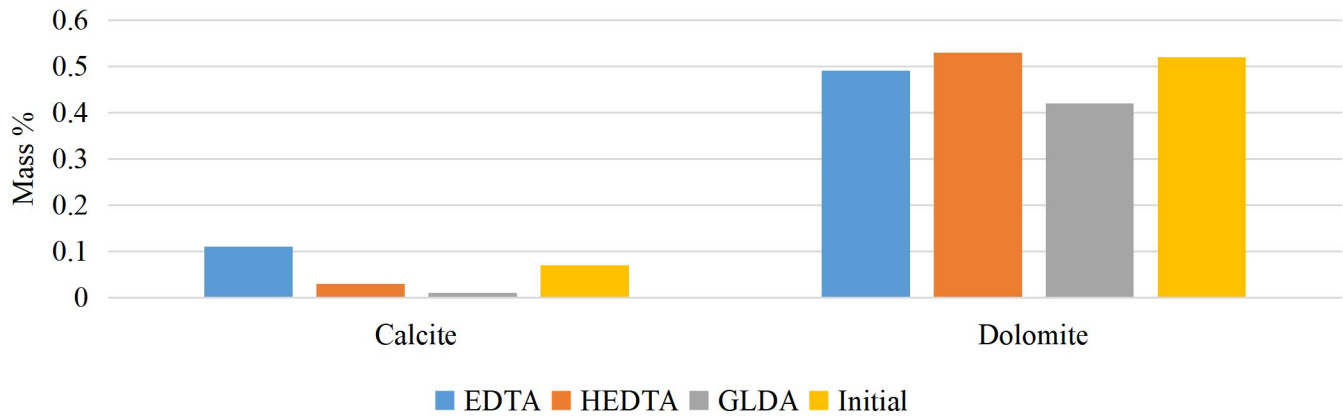

Figure 4—Calcium deportment in Guelph dolomite before and after reaction with chelating agents.
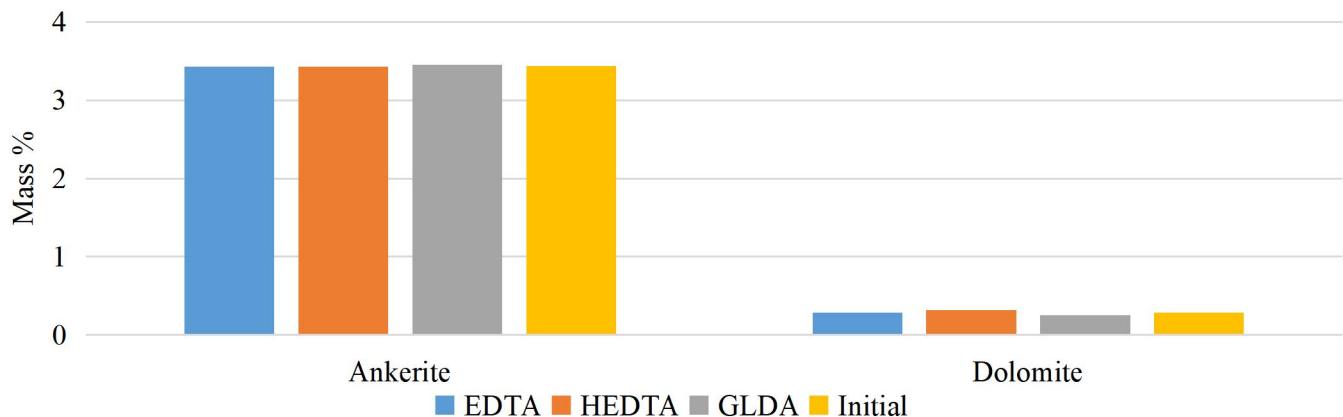

Figure 5—Magnesium deportment in Guelph dolomite before and after reaction with chelating agents.

Mineral Analysis. Figure 6 presents the mineral mass changes in the Guelph dolomite sample after treatment with the three chelating agents. The analysis revealed a notable increase in the relative weight percentage of dolomite, which can be attributed to the dissolution of other mineral phases within the sample. Among the tested chelates, HEDTA (hydroxyethyl ethylenediamine triacetic acid) and GLDA (L-glutamic acid N,N-diacetic acid) demonstrated significant effectiveness in dissolving calcite.

Furthermore, both EDTA (ethylenediaminetetraacetic acid) and HEDTA were observed to cause partial dissolution of ankerite, albeit to a limited extent. This finding aligns with the earlier discussion on the mineral-specific reactivity of chelating agents. In contrast, the relative weight of quartz increased, indicating its resistance to dissolution during the acidizing process. This behavior is consistent with the inert nature of quartz under the experimental conditions.

These results highlight the selective dissolution capabilities of chelating agents, with GLDA and HEDTA showing particular efficacy in targeting calcite, while EDTA and HEDTA exhibited minor reactivity toward ankerite. The persistence of quartz further underscores the importance of mineralogical composition in determining the outcomes of acidizing treatments.
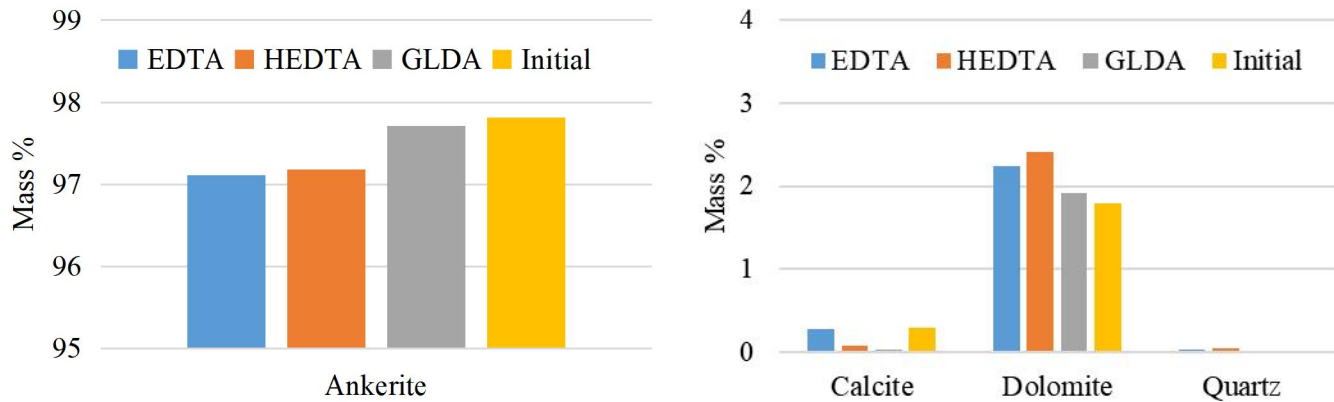
Figure 6—Mineral mass in Guelph dolomite when reacted with chelating agents.

Mineral Locking Analysis. Mineral locking refers to the intergrowth or association of different mineral phases within a rock matrix. Figure 7 illustrates the locking of calcite with ankerite and dolomite in the Guelph dolomite core sample. The analysis revealed that GLDA (L-glutamic acid N,N-diacetic acid) and HEDTA (hydroxyethyl ethylenediamine triacetic acid) were highly effective in breaking down the mineral locking between calcite and ankerite/dolomite. In contrast, EDTA (ethylenediaminetetraacetic acid) showed negligible effectiveness in disrupting these mineral associations. This finding underscores the potential of GLDA and HEDTA as effective agents for dolomite acidizing treatments.
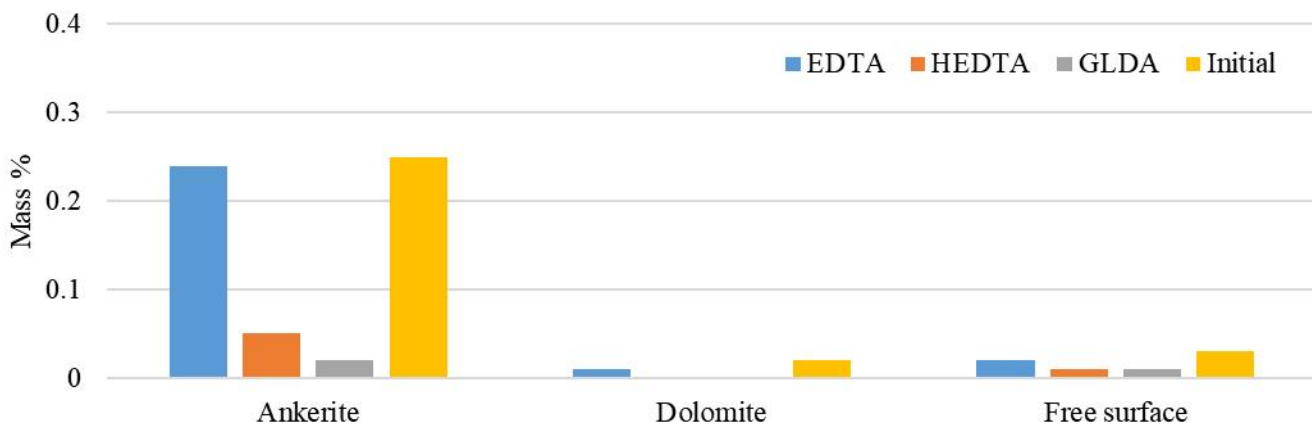

Figure 7—Calcite Mineral Locking in Guelph dolomite before and after reaction with chelating agents.

Dolomite, on the other hand, was primarily locked with ankerite but also existed as free mineral surfaces, as depicted in **Figure 8.** Since dolomite exhibited minimal solubility in the presence of all three chelating agents, its relative mineral mass increased due to the dissolution of other minerals, particularly calcite (as discussed in **Figure 9**). The dissolution of calcite not only contributed to the increase in dolomite's relative mass but also enhanced the free surface area of dolomite, potentially improving permeability and fluid flow pathways within the rock matrix.

Ankerite, which was locked with calcite, dolomite, and quartz, showed no significant change in its mineral associations after treatment with the chelating agents (Figure 9). This observation is consistent with the insolubility of ankerite under the experimental conditions, further highlighting the mineral-specific reactivity of the tested chelates.
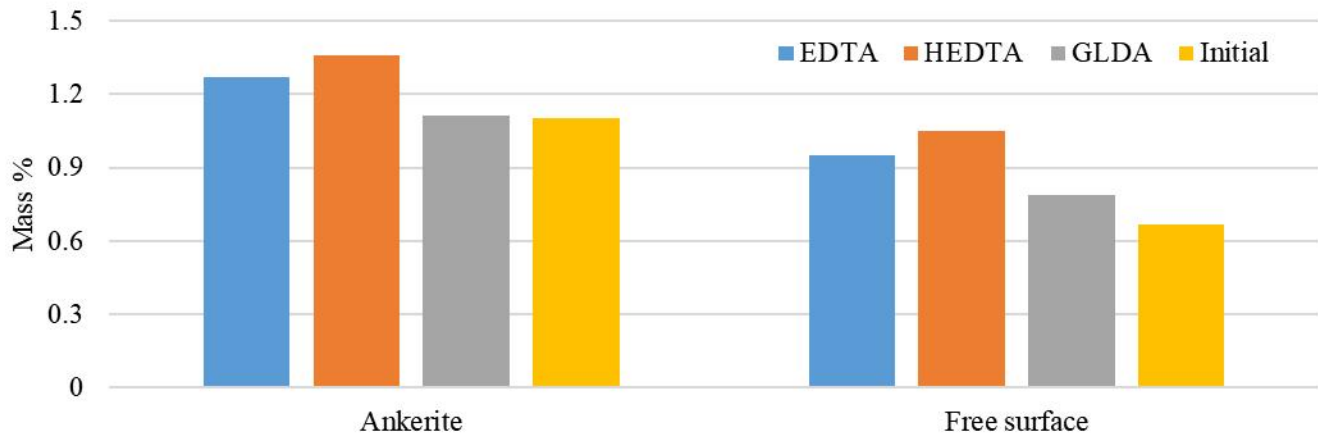
Figure 8—Dolomite Mineral Locking in Guelph dolomite when reacted with chelating agents.
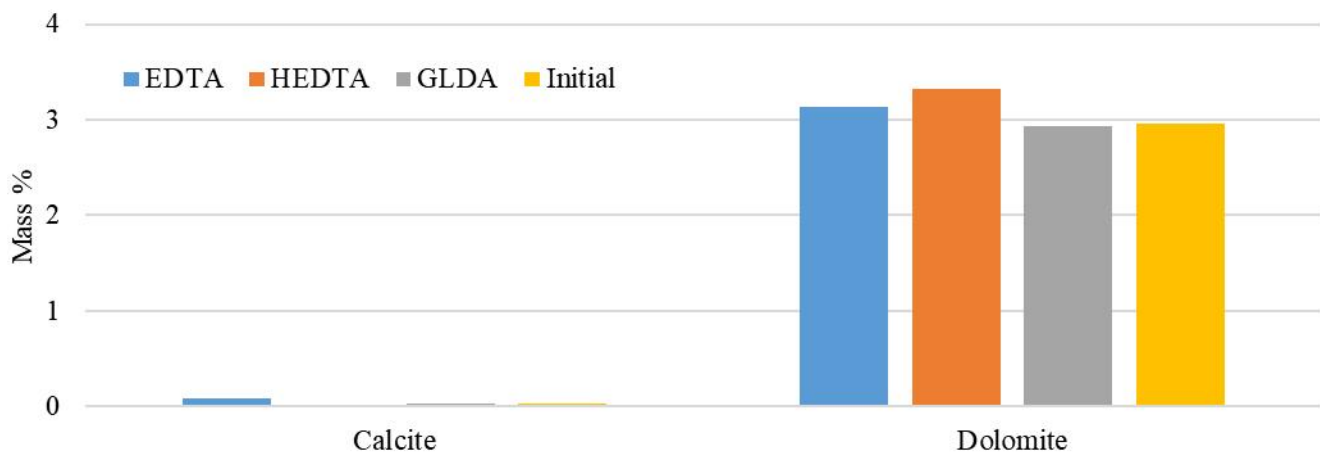

Figure 9—Ankerite Mineral Locking in Guelph dolomite when reacted with chelating agents.

Grain Size Distribution Analysis. **Figures 10** through **12** illustrate the grain size distribution of key minerals in the Guelph dolomite core sample before and after acidizing. The size ranges selected for analysis were based on the predominant grain sizes of each mineral within the sample. Ankerite exhibited the largest grain sizes, indicating the presence of coarse-grained ankerite within the core sample.

As shown in Figure 10, no significant change was observed in the number of ankerite grains after acidizing, confirming its resistance to dissolution by the tested chelating agents. This finding aligns with previous observations regarding the insolubility of ankerite under the experimental conditions.

In contrast, Figure 11 demonstrates a noticeable reduction in the number of calcite grains, particularly in the presence of GLDA (L-glutamic acid N,N-diacetic acid) and HEDTA (hydroxyethyl ethylenediamine triacetic acid). This reduction confirms the effective dissolution of calcite by these chelating agents, further supporting their potential for targeted mineral dissolution in carbonate formations.

However, as depicted in Figure 12, only a minimal change was observed in the quantity of dolomite grains, indicating limited reactivity of the chelates with dolomite. This result is consistent with the earlier findings that dolomite remains largely unaffected by the tested chelating agents.
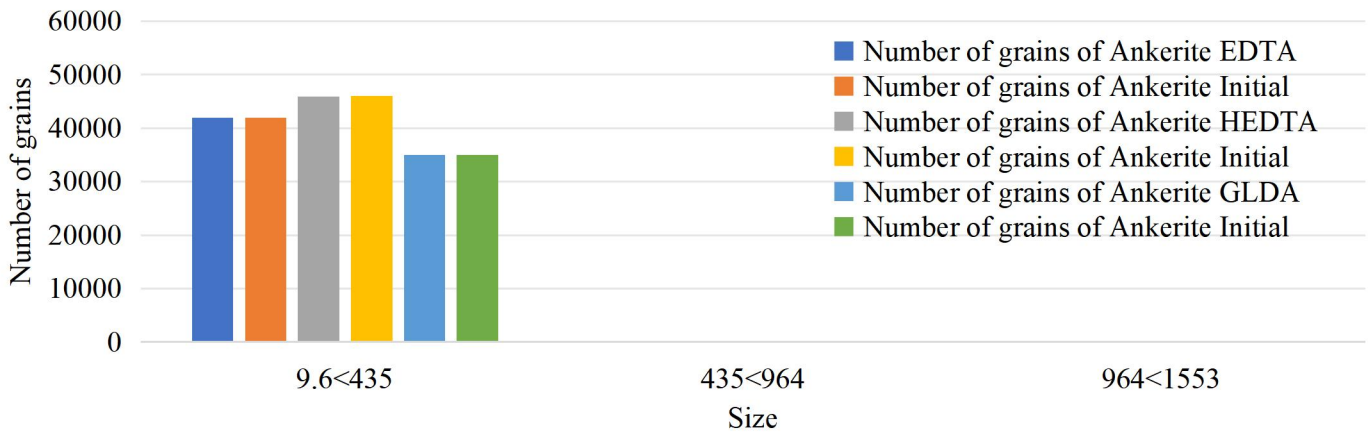
Figure 10—Ankerite grain size distribution in Guelph dolomite prior to and after chelating agent reaction.
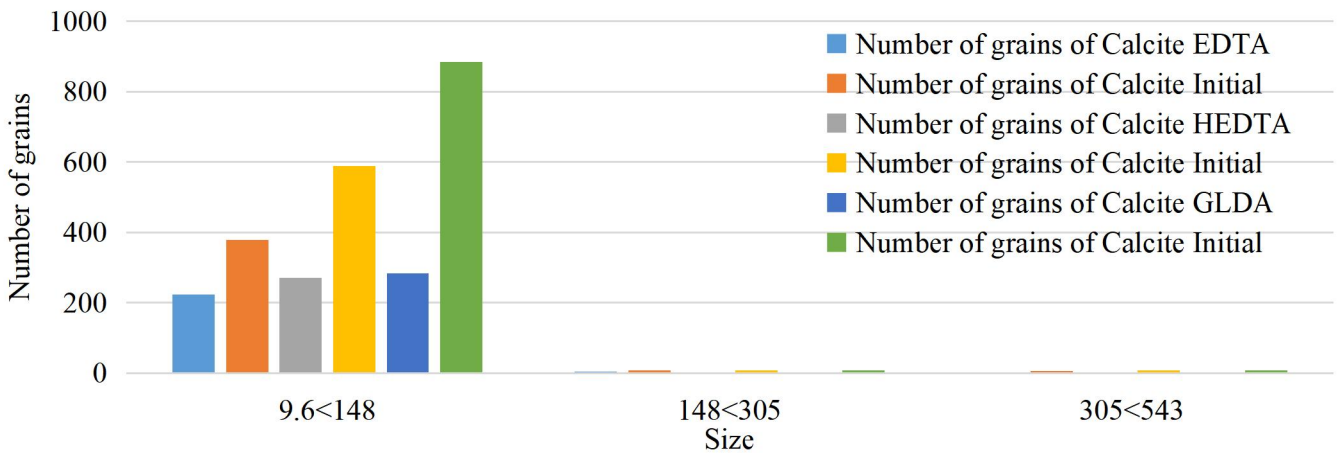

Figure 11—Calcite grain size distribution in Guelph dolomite prior to and after chelating agent reaction.
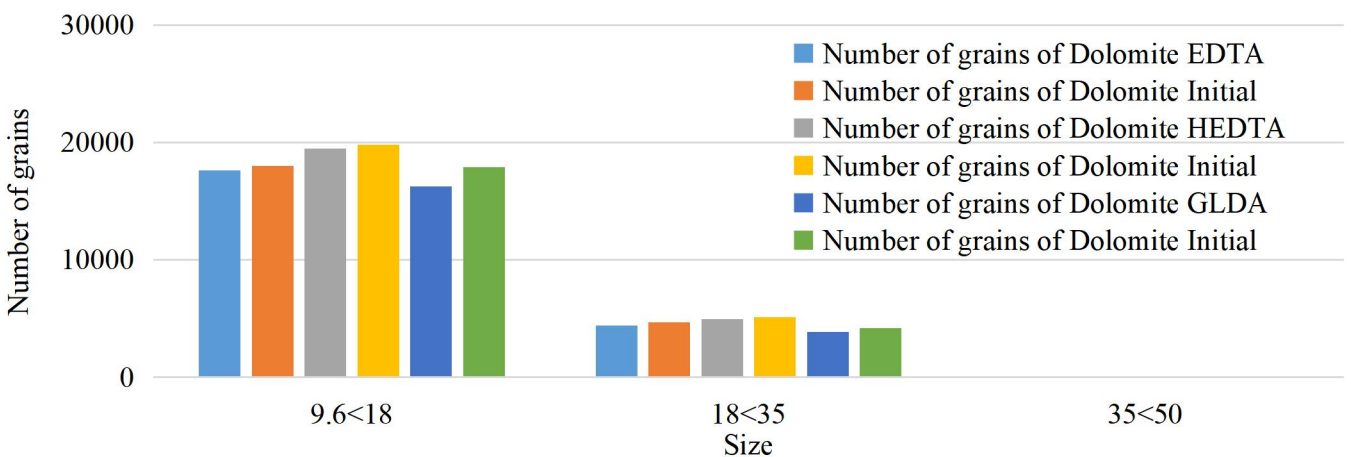

Figure 12—Dolomite grain size distribution in Guelph dolomite prior to and after chelating agent reaction.

Panorama Analysis. **Figures 13** through **18** provide a detailed visual representation of dissolution patterns and pore space formation in the Guelph dolomite core samples following treatment with the chelating agents. In these images, the ankerite matrix is highlighted in orange, while calcite is represented in pink. The analysis reveals the formation of new pore spaces and the partial disintegration of the mineral matrix in all acidized

samples, demonstrating the effectiveness of the chelating agents in altering the rock's microstructure. The rectangular markers in **Figures 13** through **18** highlight specific areas where dissolution or changes in the rock matrix occurred after acidizing. These markers provide a clear visual comparison between the pre- and post-acidizing conditions, enabling a detailed assessment of the chelating agents' effectiveness.

EDTA-Treated Sample. Figures 13 and 14 display the general overview and close-up images of the core samples treated with EDTA (ethylenediaminetetraacetic acid). Figures 13(a) and 14(a) depict the core samples before acidizing, showing the intact mineral matrix with no visible dissolution. In contrast, Figures 13(b) and 14(b) illustrate the same samples after treatment with EDTA (ethylenediaminetetraacetic acid). The rectangular markers in Figures 13 and 14 indicate areas where dissolution has occurred, primarily affecting calcite and creating new pore spaces. While some dissolution is evident, the extent of matrix alteration is relatively limited compared to the other chelating agents.
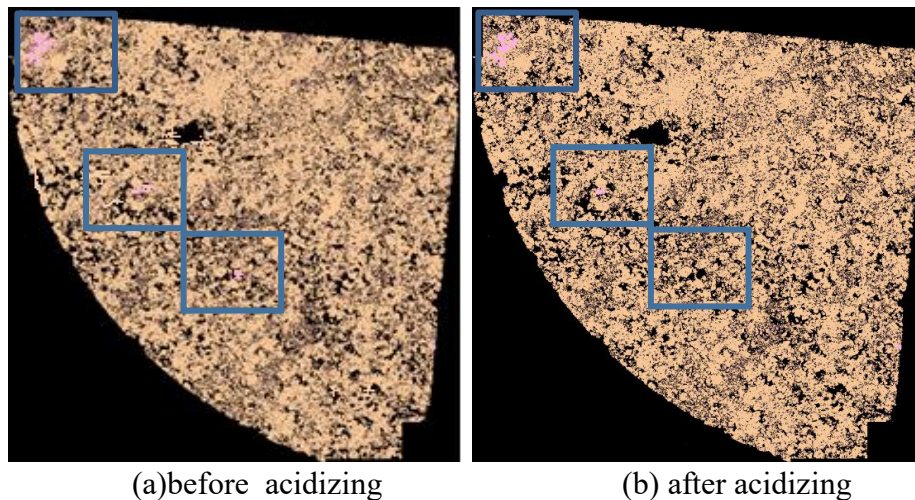

(a)before acidizing   (b) after acidizing

Figure 13—Calcite and ankerite dissolution after reaction with EDTA on Dolomite A.

(a)before acidizing   (b) after acidizing
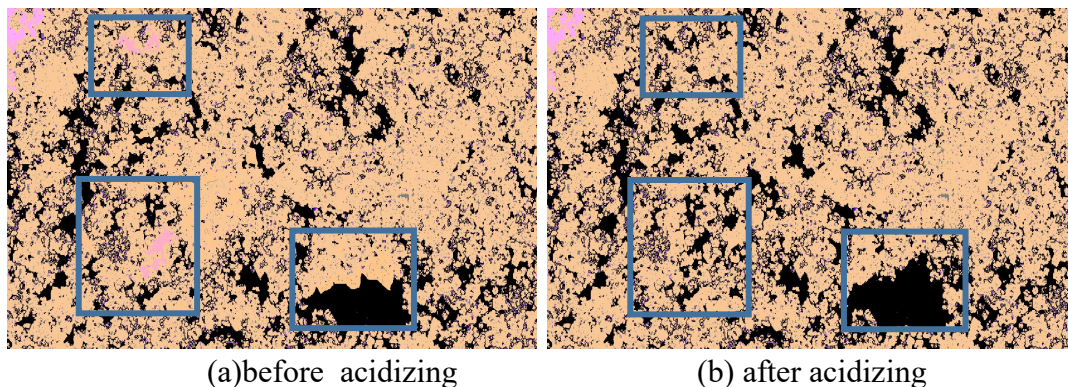
Figure 14—Calcite and ankerite dissolution after reaction with EDTA on Dolomite B.

HEDTA-Treated Sample. Figures 15 and 16 illustrate the panoramic and detailed views of the core sample after reaction with HEDTA (hydroxyethyl ethylenediamine triacetic acid). The images show more pronounced dissolution of calcite and the creation of additional pore spaces, highlighting HEDTA's effectiveness in enhancing rock permeability.

Figures 15(a) and 16(a) show the samples before acidizing, while Figure 15(b) and 16(b) display the samples after treatment with HEDTA (hydroxyethyl ethylenediamine triacetic acid). The rectangular markers in Figures 15 and 16 point to areas where significant dissolution of calcite has taken place, resulting in the formation of new pore spaces and enhanced connectivity within the rock matrix.
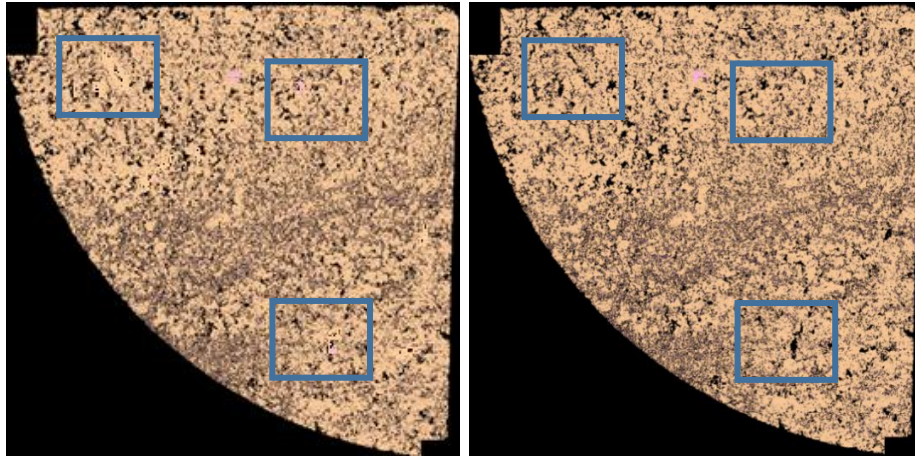
Figure 15—Calcite and ankerite dissolution after reaction with HEDTA on Dolomite A.
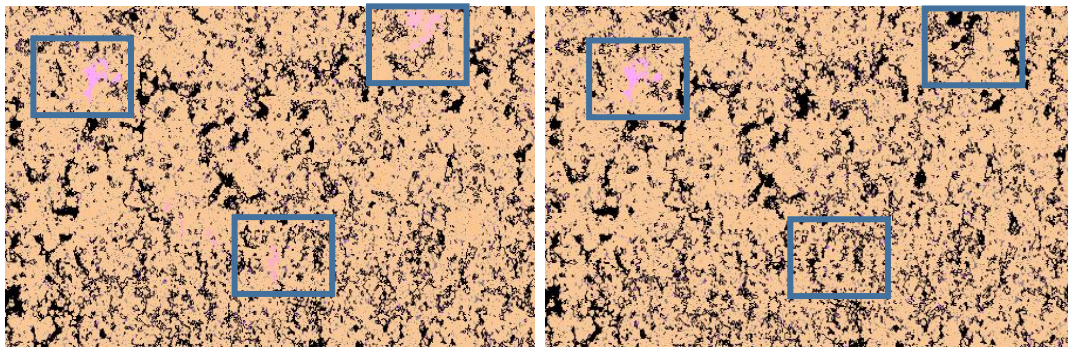

Figure 16—Calcite and ankerite dissolution after reaction with HEDTA on Dolomite B.

GLDA-Treated Sample. Figures 17 and 18 present the overall panorama and close-up images of the core sample treated with GLDA (L-glutamic acid N,N-diacetic acid). The dissolution of calcite and the formation of new pore spaces are most evident in these images, underscoring GLDA's superior performance in matrix alteration and pore network development.

Figures 17(a) and 18(a) present the samples before acidizing, and Figures 17(b) and 18(b) show the samples after treatment with GLDA (L-glutamic acid N,N-diacetic acid). The rectangular markers in Figures 17(b) and 18(b) highlight extensive dissolution of calcite and the creation of a well-developed pore network, demonstrating GLDA's superior performance in matrix alteration and permeability enhancement.
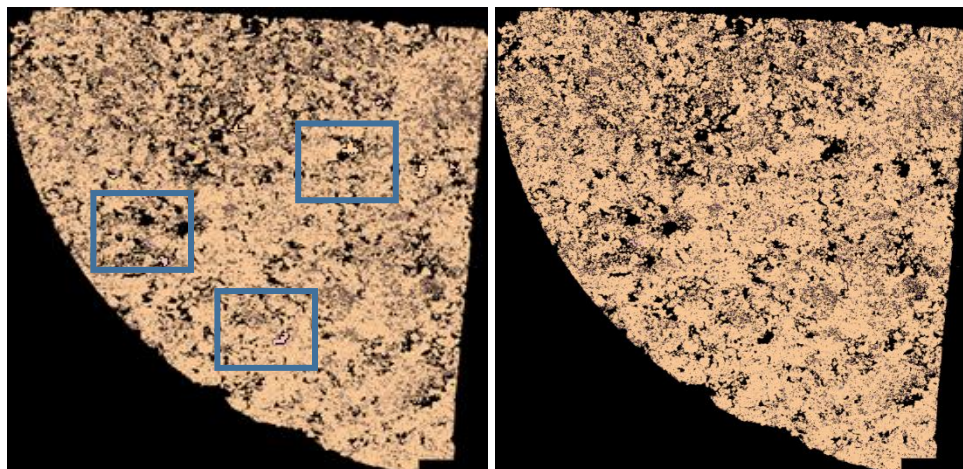

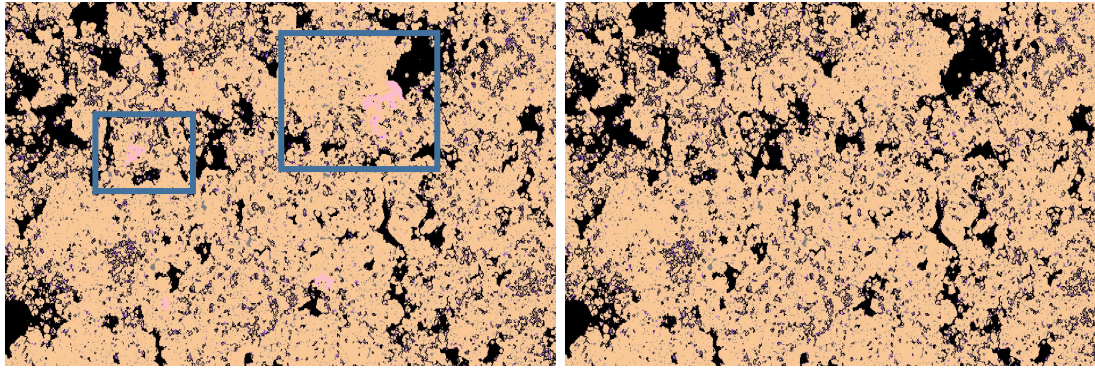**Figure 17—Calcite and ankerite dissolution after GLDA reaction.**

Figure 18—Calcite and ankerite dissolution after GLDA reaction

In summary, the panorama analysis confirms that all three chelating agents-EDTA, HEDTA, and GLDA-were effective in generating new pore spaces within the dolomite core samples. However, GLDA and HEDTA demonstrated significantly greater efficacy in dissolving calcite and enhancing pore connectivity compared to EDTA. These findings highlight the potential of GLDA and HEDTA as effective agents for acidizing treatments in carbonate reservoirs.

Porosity Distribution Analysis. **Table 2** presents the pore size distribution in the dolomite core sample, categorized into tiny (9.6-30 µm), medium (30-67 µm), and large (67-146 µm) pores, before and after treatment with the chelating agents. The results highlight the effectiveness of each chelate in enhancing porosity through the creation of new pore spaces, which is critical for improving reservoir permeability and hydrocarbon recovery.

Overall Porosity Enhancement. HEDTA generated the highest total number of new pore spaces, with 3,047 pores, demonstrating its superior ability to enhance porosity in dolomite formations. GLDA produced 2,112 new pore spaces, indicating its strong potential for reservoir stimulation, though slightly less effective than HEDTA. While EDTA resulted in only 543 new pore spaces, showing limited effectiveness in porosity enhancement.

Pore Size-Specific Performance. HEDTA created 2,743 new tiny pores, while GLDA produced 1,947. This suggests HEDTA's greater effectiveness in generating smaller pores, which can enhance permeability in tight carbonate reservoirs. HEDTA also demonstrated strong performance in creating medium-sized pores, further contributing to its overall porosity enhancement. GLDA outperformed HEDTA in the formation of larger pore spaces, creating a significant number of large voids. In contrast, HEDTA contributed only two large pores, highlighting GLDA's unique capability to develop larger flow pathways, which are essential for improving fluid connectivity in the reservoir.

Table 2—Initial and final pore size distribution of Dolomite formation.

| Pore size (µm) | Number of pore spaces | | | | | | | | |
| | Reaction with HEDTA | | | Reaction with EDTA | | | Reaction with GLDA | | |
	Initial	EDTA	New pores	Initial	HEDTA	New pores	Initial	GLDA	New pores
9.6<30	46013	48756	2743	46560	47031	471	49095	51042	1947
30<67	417	718	301	458	527	69	502	656	154
67<146	16	18	2	16	19	3	25	36	11
Total	46445	49492	3047	47034	47577	543	49622	51734	2112

HEDTA emerged as the most effective chelating agent for overall porosity enhancement in the dolomite sample, with a total increase of 3,047 new pore spaces. However, GLDA demonstrated superior performance in creating larger pore spaces, which are critical for enhancing fluid flow in carbonate reservoirs. These findings underscore the importance of selecting the appropriate chelating agent based on the desired pore size distribution and reservoir characteristics to optimize stimulation treatments.

Particle Size Distribution. **Figure 19** presents the distribution of tiny, medium, and large particles in Guelph dolomite samples before and after acidification with the tested chelating agents. The results demonstrate that all chelates effectively preserved a significant portion of solid particles while simultaneously dissolving targeted minerals, thereby enhancing pore space and overall porosity. This dual capability highlights the chelates' ability to balance mineral dissolution with particle integrity preservation, which is critical for maintaining reservoir stability during acidizing treatments.

EDTA dissolved a total of 3,879 particles, including 235 particles (47-199 µm), 137 particles (199-520 µm), 73 particles (520-985 µm), and 11 particles (985-1590 µm), as shown in Figure 19(c). The dissolved minerals primarily included ankerite and calcite, which are the dominant minerals in the dolomite matrix.

HEDTA dissolved a similar total of 4,549 particles. GLDA demonstrated superior performance, dissolving 4,010 tiny particles. It outperformed both HEDTA and EDTA in dissolving medium and large-sized particles, making it the most effective chelate for creating clean pore networks in dolomite formations.

GLDA emerged as the most effective chelating agent for acidifying dolomite formations, as it dissolved the highest number of particles across all size ranges. This capability not only enhances porosity but also improves permeability by creating well-connected pore networks. The results, summarized in **Table 3**, underscore the importance of selecting the appropriate chelating agent based on the desired particle size distribution and mineral dissolution targets for optimal reservoir stimulation.

Table 3—Number of particles in Guelph dolomite sample before and after reaction with chelating agents.

| Pore size (µm)	Number of particles								
	Reacted with EDTA			Reacted with HEDTA			Reacted with GLDA		
	Initial	Reacted	Dissolved	Initial	Reacted	Dissolved	Initial	Reacted	Dissolved
9.6< 47	47874	43995	-3879	56012	51911	-4101	44428	40418	-4010
47< 199	3778	3543	-235	4374	4085	-289	3343	3024	-319
199< 520	587	440	-147	458	354	-104	455	291	-164
520< 985	189	116	-73	125	81	-44	139	62	-77
985< 1590	57	46	-11	75	64	-11	96	80	-16
Total	52485	48140	-4345	61044	56495	-4549	48461	43875	-4586
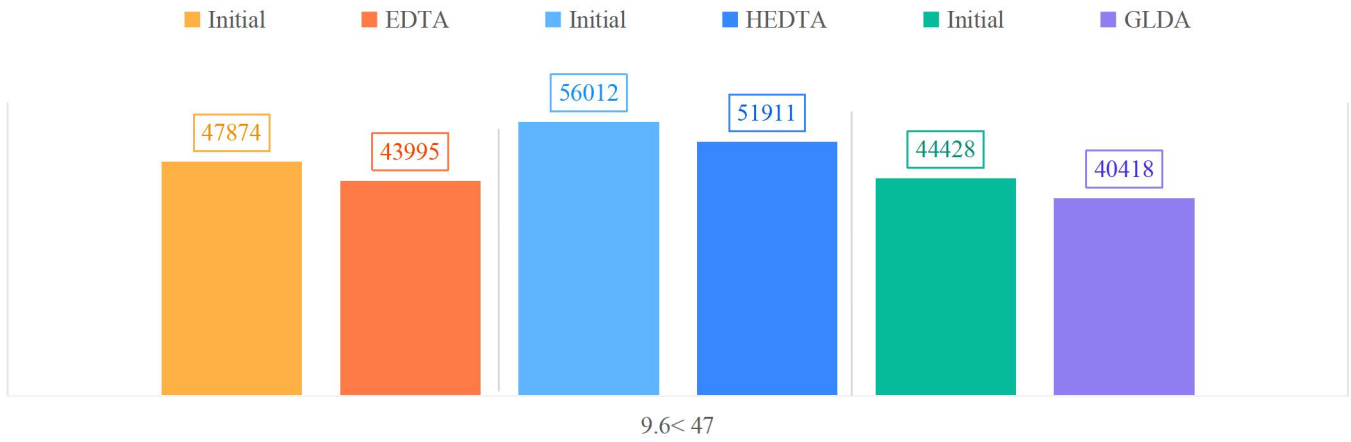
(a) Tiny particles
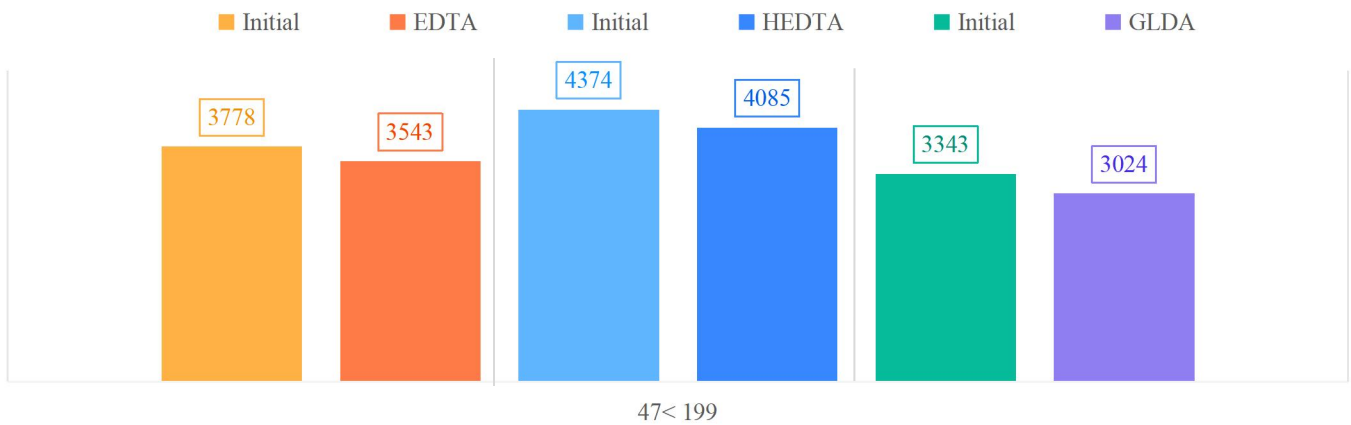
(b) Medium particles
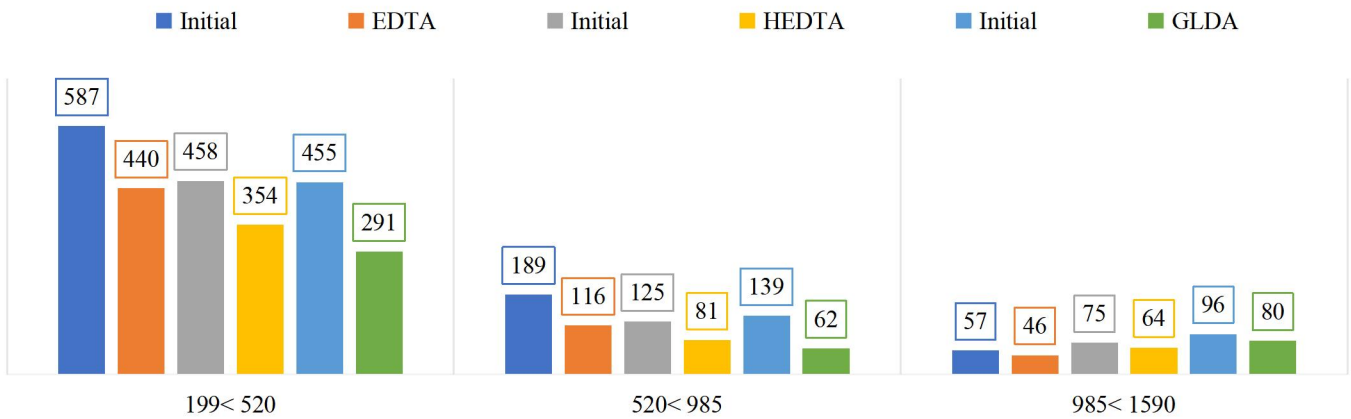
(c) Large particles

Figure 19—Number of particles in the sample of Guelph dolomite before and after treatment with chelating agents.
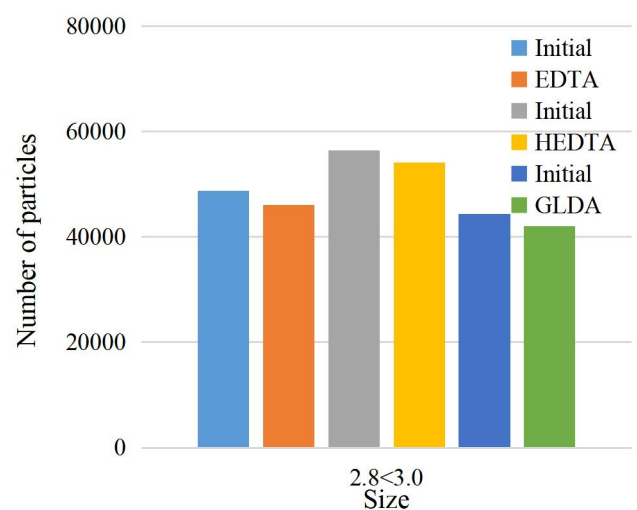
Particle Density Distribution Analysis. **Figure 20** illustrates the density distribution of particles in the Guelph dolomite sample, providing insights into the dissolution behavior of the chelating agents based on mineral density. The sample is predominantly composed of ankerite, which has a density of approximately 2.97 g/cm³, along with other minerals such as calcite (density: 2.71 g/cm³) and heavier mineral phases.
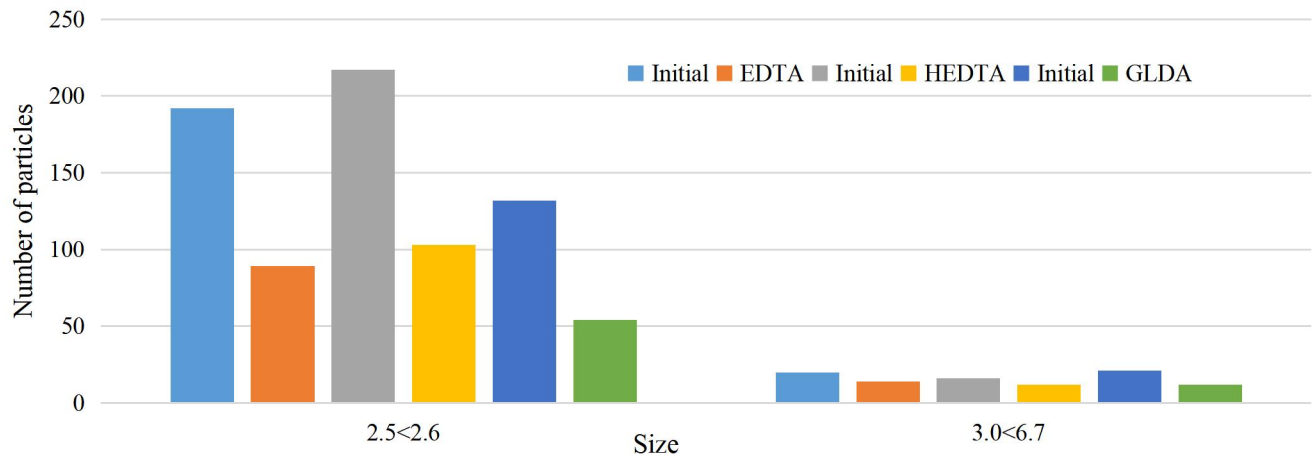
(a) Heavier minerals
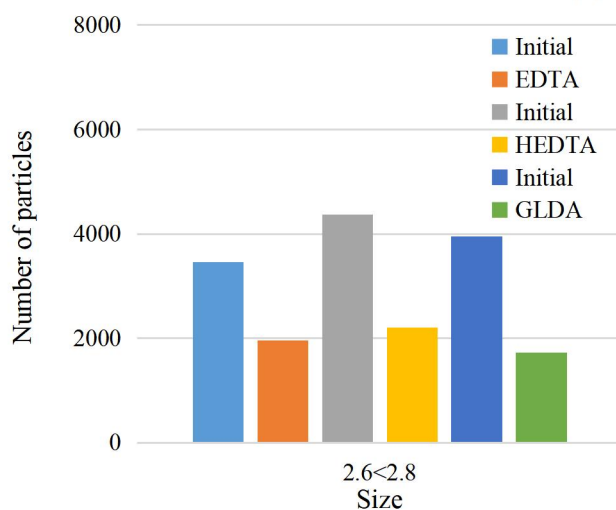
(b) Calcite

(c) Ankerite

Figure 20—Distribution of particle density in Guelph dolomite before and after treatment with chelating chemicals.

Heavier Minerals. Figure 20(a) shows minimal dissolution of particles in the higher density range (3.0−6.7 g/cm³), indicating that the chelating agents were less effective in dissolving heavier mineral phases. This suggests that the dissolution process is highly dependent on mineral density, with lighter minerals like calcite being more susceptible to chelate-induced dissolution.

Calcite. The chelating agents demonstrated high efficacy in dissolving calcite, as evidenced by the significant reduction in the number of particles within this density range (Figure 20(b)). This finding aligns with earlier results, highlighting the selective dissolution of calcite by HEDTA, GLDA, and, to a lesser extent, EDTA.

Ankerite. As shown in Figure 20(c), the majority of particles fall within the density range of 2.8−3.0 g/cm³, consistent with the presence of ankerite. The solubility of ankerite was relatively low, resulting in only a slight change in the number of particles after acidizing. This confirms the limited reactivity of the chelating agents with ankerite, as previously discussed.

The particle density distribution analysis confirms the mineral-specific reactivity of the chelating agents, with calcite showing the highest dissolution rates due to its lower density, while ankerite and heavier minerals remained largely unaffected. These findings underscore the importance of considering mineral density and composition when designing acidizing treatments for carbonate reservoirs. The results also validate the effectiveness of chelating agents like HEDTA and GLDA in selectively dissolving target minerals to enhance porosity and permeability.

Conclusion

This study investigated the effects of three chelating agents — EDTA, HEDTA, and GLDA — on Guelph dolomite core samples to evaluate their effectiveness in mineral dissolution and porosity enhancement. Key findings from the analysis are summarized as follows:

1. The initial elemental composition of the dolomite samples remained largely unchanged after acidizing, likely due to the high concentration of ankerite, which acted as an insoluble matrix mineral.
2. Calcite was effectively dissolved by HEDTA and GLDA, demonstrating their strong reactivity with this mineral. Dolomite, which was locked with ankerite, showed significant mineral locking removal when treated with GLDA and HEDTA, highlighting their ability to disrupt mineral associations and enhance pore connectivity.
3. The analysis revealed that the number of ankerite grains remained largely unchanged, consistent with its low solubility. In contrast, the number of calcite grains decreased significantly, particularly in samples treated with GLDA and HEDTA, confirming their effectiveness in dissolving calcite.
4. HEDTA emerged as the most effective chelate for enhancing porosity, generating 3,046 additional pore spaces in the dolomite formation. This underscores its potential for improving reservoir permeability.
5. All chelating agents dissolved a significant number of solid particles, with GLDA demonstrating superior performance in dissolving medium and large-sized particles. This capability makes GLDA particularly effective in creating clean, well-connected pore networks.
6. The analysis confirmed that GLDA was more effective than HEDTA and EDTA in acidifying dolomite formations, particularly in dissolving lighter minerals like calcite while preserving the integrity of denser minerals such as ankerite.

This study provides valuable insights into the mineral-specific reactivity and porosity-enhancing capabilities of chelating agents in dolomite formations. HEDTA and GLDA demonstrated superior performance in dissolving calcite, removing mineral locking, and enhancing pore connectivity, making them highly effective for carbonate reservoir stimulation. These findings highlight the importance of selecting the appropriate chelating agent based on reservoir mineralogy and desired outcomes to optimize acidizing treatments and improve hydrocarbon recovery.

Acknowledgment

Conflicting Interests

The author(s) declare that they have no conflicting interests.

References

Al-Harthy, S. 2009. Options for High-Temperature Well Stimulation. *Oil Field Review* **20**(4)L15-24.

Almubarak, T., Ng, J. H., and Nasr-El-Din, H. 2017. Oilfield Scale Removal by Chelating Agents: An Aminopolycarboxylic Acids Review. Paper presented at the SPE Western Regional Meeting, Bakersfield, California, 23-25 April. SPE-185636-MS.

Bernadiner, M. G., Thompson, K. E., and Fogler, H. S. 1992. Effect of Foams Used During Carbonate Acidizing. *SPE Prod Eng* **7**(4): 350-356. SPE-21035-PA.

Buijse, M. A. and van Domelen, M. S. 1998. Novel Application of Emulsified Acids to Matrix Stimulation of Heterogeneous Formations. *SPE Prod & Fac* **15**(3): 208-213. SPE-65355-PA.

Ettinger, R. A. and Radke, C. J. 1992. Influence of Texture on Steady Foam Flow in Berea Sandstone. *SPE Res Eng* **7**(1): 83-90. SPE-19688-PA.

Fredd, C. N. and Fogler, H. S. 1998. The Influence of Chelating Agents on the Kinetics of Calcite Dissolution. *J Colloid Interface Sci* **204**(1): 187-197.

Gdanski, R. 1998. Kinetics of Tertiary Reactions of Hydrofluoric Acid on Aluminosilicates. *SPE Prod & Fac* **13**(2): 75-80. SPE-31076-PA.

Ghommem, M., Zhao, W., Dyer, S., et al. 2015. Carbonate Acidizing: Modeling, Analysis, and Characterization of Wormhole Formation and Propagation. *Journal of Petroleum Science and Engineering* **131**(1): 18-33.

Hassan, A. M. and Al-Hashim,H. S. 2017. Evaluation of Carbonate Rocks Integrity After Sequential Flooding of Chelating Agent Solutions. Paper presented at the SPE Middle East Oil & Gas Show and Conference, 6-9 March. SPE-183760-MS.

Hoefner, M. L. 1987. Matrix Acidizing in Carbonates Using Microemulsions: The Study of Flow, Dissolution and Channeling in Porous Media. Thesis, University of Michigan, Ann Arbor, Michigan.

Maheshwari, P. and Balakotaiah, V. 2013. 3D Simulation of Carbonate Acidization with HCl: Comparison with Experiments. *SPE Prod & Oper* **28**(4): 402-413.SPE-164517-PA.

Morgenthaler, L. 2013. Technology Focus: Matrix Stimulation. *Journal of Petroleum Technology* **68**(6):1-17.

Nasr-El-Din, H. A., Al-Mutairi, S. H., Al-Jari, M., et al. 2002. Stimulation of a Deep Sour Gas Reservoir Using Gelled Acid. Paper presented at the SPE Gas Technology Symposium, Calgary, Alberta, Canada, 30 April. SPE-75501-MS.

Nasr-El-Din, H. A., Samuel, M. M., and Kelkar, S. K. 2007. Investigation of a Single-stage Sandstone Acidizing Fluid for High-Temperature Formations. Paper presented at the European Formation Damage Conference, Scheveningen, The Netherlands, 30 May. SPE-107636-MS.

Qiu, X., Zhao, W., Dyer, S. J., et al. 2011. Revisiting Reaction Kinetics and Wormholing Phenomena During Carbonate Acidizing. Paper presented at the International Petroleum Technology Conference, Doha, Qatar, 19-21 January. IPTC-17285-MS.

Shafiq, M. U. and Ben Mahmud, H. K. 2017. Sandstone Matrix Acidizing Knowledge and Future Development. *J Petrol Explor Prod Technol* **7**(4):1205-1216.

Shafiq, M. U., Ben Mahmud, H. K., Gishkori, S. N., et al. 2023. Acidizing of Conventional and Tight Sandstone Formation using Chelating Agents: Mineralogical Prospect. *Journal of Petroleum Exploration and Production Technology* **10**(1): 3587-3599.

Shafiq, M. U., H. K. Ben Mahmud, L. Wang, K. Abid, S. N. Gishkori. 2022. Comparative Elemental, Mineral and Microscopic Investigation of Sandstone Matrix Acidizing at HPHT Conditions. *Journal of Petroleum Research* **7**(3):448-458.

Shafiq, M. U., H. K. Ben Mahmud, L. Wang, M. Khan, N. Qi, K. Abid, S. N. Gishkori. 2023. Mineral Analysis of Sandstone Formation using Chelating Agents during Sandstone Matrix Acidizing. *Journal of Petroleum Research* **8**(3): 404-412.

Ward, I., Merigot, K., and McInnes, B. I. A. 2017. Application of Quantitative Mineralogical Analysis in Archaeological Micromorphology: a Case Study from Barrow Is., Western Australia. *J Archaeol Method Theory* **25**(1): 45-68.

Wilson, A. 2016. Sandstone-Acidizing System Eliminates Need for Preflush and Post-Flush Stages. *J Pet Technol* **68**(6): 59-60. SPE-0616-0059-JPT.